Asian Journal of Science and Applied Technology
ISSN: 2249-0698 (P) Vol.3 No.2, 2014, pp.12-24

DOI: https://doi.org/10.51983/ajsat-2014.3.2.795

An Investigation on Instantaneous Workability Behavior of Aluminium SiC Air Quenched Powder Composites During Cold Upsetting

M. Prabhakar [1], T. Ramesh[2], R. Narayanasamy[3] and V. Anandakrishnan[4]
[1] Professor, Department of Mechanical Engineering, TRP Engineering College,
Trichirappalli, Tamil Nadu, India
[2] Asst. Professor, Department of Mechanical Engineering,
[3] Professor, [4] Asst. Professor, Department of Production Engineering,
National Institute of Technology, Trichirappalli, Tamil Nadu, India
E-mail:mprabha2000@rediffmail.com
(Received 16 July 2014; Revised 2 August 2014; Accepted 23 August 2014; Available online 29 August 2014)

Abstract **- Strain hardening of a material is an important phenomenon, which is required to study the plastic deformation of any material and also is an important parameter in the study of workability criteria of metals. The present investigation has been undertaken to evaluate the instantaneous strain hardening behaviour experienced during the cold working of sintered aluminium SiC composites from 0 to 15% under various stress state conditions namely uniaxial, plane and triaxial. Sintered preforms with three different aspect ratios namely 0.38, 0.76 and 1.19 with for different per cent of SiC contents ranging from 0 to 15% were prepared and cold forged. The results were obtained for each aspect ratios and SiC contents at different stress state conditions.**
Keywords: **Upsetting; Strain hardening exponent; Strength coefficient; Powder Metallurgy; Triaxial stress**

I. INTRODUCTION

Powder metallurgy (P/M) process provides several advantages when comparing with conventional manufacturing process. It can provide a reasonable improvement in specific strength, stiffness and wear resistant, compared with monolithic alloys. At present, the powder metallurgy components are being widely used for sophisticated industrial applications. The worldwide popularity of powder metallurgy lies in the ability of this technique to produce such complex shapes with exact dimensions at a high rate of production with low cost prices. Frequently, this technology is used for material systems that are hard to machine such as tungsten or molybdenum or very much difficult to cast due to detrimental solidification behavior of material chosen.

Abdel-Rahman and Sheikh [1] discussed workability criterion of powder metallurgy compacts and they investigated the effect of the relative density on the forming limit of P/M compacts in upsetting. They proposed a workability factor (β) for describing the effect of the mean stress and the effective stresses with the help of two theories and they discussed the effect of relative density.

Narayanasamy and Pandey [2] performed an excellent work on the strain hardening behaviour of the powder metallurgy composites. They evaluated the work hardening characteristics of sintered aluminium–iron composite preform conducting experimental works under uniaxial stress state conditions and studied the strength coefficient value for various iron particle sizes.

Narayanasamy and Pandey [3] investigated the evaluation of cold upset-forming and densification features in aluminium–3.5% alumina sintered powder preforms and they concluded that the preforms possessing lower initial aspect ratios have shown enhanced densification compared to preforms of higher initial aspect ratios, subject to the condition where the initial preform densities maintained constant. Further they studied the effect of Poisson's ratio with respect to the fractional theoretical density attained exhibited three distinct stages, namely, a steep rise, a steady state, followed by a rapid rise approaching to value of 0.5 in the close vicinity of the theoretical density [4].

Narayanasamy and Ramesh investigated the workability criteria under triaxial conditions for Aluminum and iron compacts with various particle sizes and they found the triaxial stress conditions with various aspect ratios [5], the same author investigated the strain hardening exponent and strength coefficient for the same combination composites [6].

Sridhar and fleck [7] did their experiment on triaxial test on cold compaction behavior of lead shot with steel reinforcement as well as Aluminium and 40% silicon carbide powder under hydrostatic loading conditions and they found the shape deformations and hardening parameters along the loading directions.

Li and Mohamed [8] investigated the creep behavior on 10vol % SiC with 2124Aluminium composites. Z. Lin [9] also investigated with the same aluminium combination with 5vol % SiC additions and investigated the creep behavior of the composites.

In this paper, a complete investigation deformation behavior of aluminium powder metallurgy composites with various percent of SiC contents ranging from 0 to 15% for the various stress state conditions namely, uniaxial, plane and triaxial conditions with three different aspect ratios were performed. The formability stress index found for various per cent of SiC content of preforms for various stress state conditions were calculated and plotted against the axial strain. From the plot it is observed that the addition of SiC particles in the aluminium powder preforms do have great changes in the formability stress index 'β' and axial strain.

Nomenclature

D_b	bulged diameter
D_c	contact diameter
D_0	initial diameter
H_f	height of the compact at fracture
H_0	initial height of compact

Greek letters

α	Poisson's ratio
ε_{eff}	effective strain component
ε_r	radial strain component
ε_z	axial strain component
ε_θ	hoop strain component
σ_{eff}	effective stress component
σ_m	mean stress
σ_r	radial stress component
σ_z	axial stress component
σ_θ	hoop stress component

II. THEORETICAL INVESTIGATIONS

The mathematical expressions used and proposed for the determination of various upsetting parameters for various stress state conditions are discussed below.

A. Uniaxial stress state and plane stress state conditions

In the compression of P/M part, under frictional conditions, the average density is increased. Friction enhances densification and at the same time decreases the height reduction at fracture. The state of stress in a homogeneous compression process is as follows.
According to Abdel-Rahman and Sheikh [1]:

$$\sigma_z = -\sigma_{eff},\ \sigma_r = \sigma_\theta = 0 \quad (1)$$

where σ_z is the axial stress, σ_{eff} is the effective stress, σ_r is the radial stress and σ_θ is the hoop stress.

$$\sigma_m = \frac{\sigma_Z}{3} \quad (2)$$

where σ_m is the mean or hydrostatic stress and the strain state is

$$\varepsilon_Z = \ln\left(\frac{h_0}{h_f}\right) \quad (3)$$

and

$$\varepsilon_\theta = \ln\left(\frac{2D_b^2 + D_c^2}{3D_o^2}\right) \quad (4)$$

where D_b is the bulged diameter of compacts; D_c is the contact diameter of compacts and; D_0 is the initial diameter of compacts.

When the compression continues, the final diameter increases and the corresponding hoop strain, which is tensile in nature, also increases until it reaches the fracture limit. The associated flow characteristics for porous materials under plane stress state condition can be expressed as

$$d\varepsilon_z = d\lambda(\sigma_z - \nu\sigma_\theta) \quad (5)$$

$$d\varepsilon_\theta = d\lambda(\sigma_\theta - \nu\sigma_z) \quad (6)$$

where $d\varepsilon_z$ is the plastic strain increment in the axial direction, $d\varepsilon_\theta$ is the plastic strain increment in the hoop direction, $d\lambda$ is the constant.
As an evidence of experimental investigation implying the importance of the spherical component of the stress state on fracture called a formability stress index 'β' which is given by:

$$\beta = \frac{3\sigma_m}{\sigma_{eff}} \quad (7)$$

This index determines the fracture limit

According to Narayanasamy and Pandey [4], the state of stress in a plane stress condition is as follows:

$$\sigma_{eff} = (0.5 + \alpha)[3(1 + \alpha + \alpha^2)]^{1/2}\sigma_z \quad (8)$$

where σ_{eff}-is the effective stress, α is the Poisson's ratio = $(\varepsilon_\theta/2\varepsilon_z)$
Since, the radial stress σ_r is zero at the free surface it follows from the flow rule that,

$$\sigma_\theta = \left(\frac{1+2\alpha}{2+\alpha}\right)\sigma_Z \quad (9)$$

Further using the values of σ_z and σ_θ, the hydrostatic stress (σ_m) can be calculated as follows:

$$\sigma_m = \frac{1}{3}\left[\sigma_Z \pm \sigma_\theta\right] \quad (10)$$

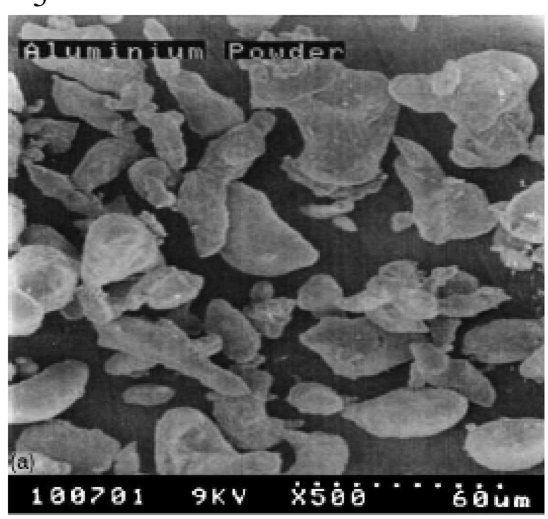

Fig. 1. SEM photo of the aluminium powder.

(a) (b) (c)

Fig. 2. (a) Al + 5% SiC specimen- SiC particle size 180 microns- macrostructure (b) Al + 10% SiC specimen- SiC particle size 180 microns- macrostructure (c) Al + 15% SiC specimen- SiC particle size 180 microns- macrostructure

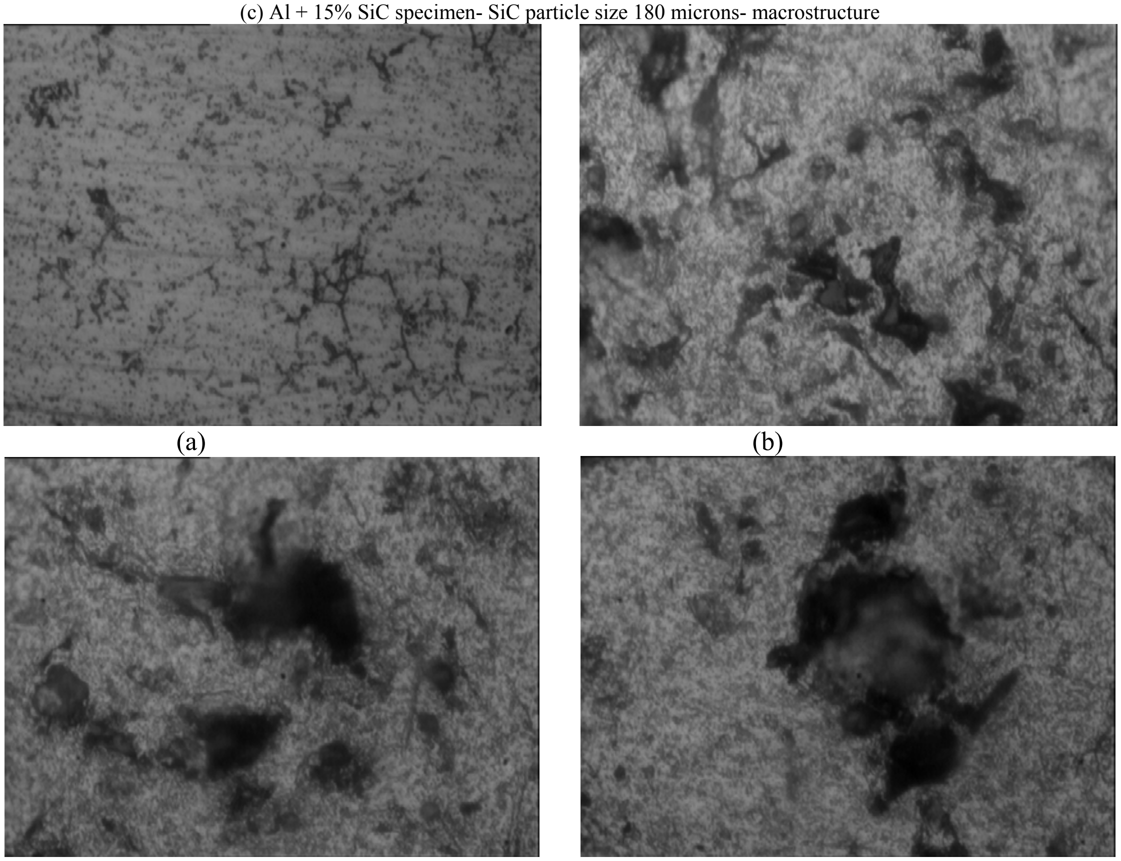

(a) (b) (c) (d)

Fig. 3. Microstructure of (a) pure Aluminium (b) pure Aluminium and 5% SiC addition (c) pure Aluminium and 10% SiC addition (d) pure Aluminium and 15% SiC addition

B. Triaxial stress state condition

According to Narayanasamy and Ponalagusamy [14] the state of stress in triaxial stress state condition is as follows:

$$\alpha = \frac{(2+R^2)\sigma_\theta - R^2(\sigma_Z + 2\sigma_\theta)}{(2+R^2)\sigma_Z - R^2(\sigma_Z + 2\sigma_\theta)} \qquad (11)$$

where R is the relative density.

From the Eq. (11) for the known values of α, R and σ_z, the hoop stress component (σ_θ) can be determined as follows:

$$\sigma_\theta = \left(\frac{2\alpha + R^2}{2 - R^2 + 2R^2\alpha}\right)\sigma_Z \qquad (12)$$

At triaxial stress state condition, the relative density (R) of the compacts plays a vital role in the determination of the hoop stress component (σ_θ). Since $\sigma_r = \sigma_\theta$ in the case of triaxial stress stated condition, the hydrostatic stress (σ_m) is given by

$$\sigma_m = \frac{\sigma_1 + \sigma_2 + \sigma_3}{3} = \frac{1}{3}(\sigma_Z + 2\sigma_\theta) \qquad (13)$$

III. EXPERIMENTAL

Atomized aluminium and SiC powders of the characteristic stated in the Table 1 was procured and analyzed for its purity. The purity level of the aluminium and SiC powders was found to be 99.7 and 99.62%, respectively. Fig. 1 show the SEM photographs of aluminium powder. The compacts were prepared from aluminium and SiC powders with different aspect ratios at the compacting pressure range of 200–225MPa (410-485 MPa) in order to obtain the initial preform density ranging from 0.85 to 0.92 of the theoretical value. The powder metal compacts were prepared by blending aluminium and SiC powders of different SiC contents (0–15%) with SiC powders of particle size namely 180µm. The ceramic coating was applied over the surface of the compacts to protect them from oxidation during sintering. The ceramic-coated compacts were sintered in an electric muffle furnace at 550 °C for period of 90 min and air quenched by switching off the furnace power supply and opened to the room temperature.

TABLE I CHARACTERISTICS OF ALUMINIUM AND SIC POWDERS

Sieve analysis (aluminium)		Characteristics of aluminium powder	
Sieve number (µm)	wt.% retained		
+106	0.26	Apparent density (g cm^{-3})	1.030
+90	2.54	Flow rate, S (by Hall flow meter) (50 g^{-1})	32.00
+75	14.73	Compressibility at a pressure	
+63	17.58	of 300MPa (g cm^{-3})	2.344
+53	24.86		
+45	12.33		
+38	6.27		
−38	21.42		
SiC particle size 180 µm			

The sintered preforms were cleaned from the sand particles and the dimensional measurement made before and after each deformation. The deformation of the compact was carried out between two flat open dies hardened to Rc 50–55 and tempered to Rc 46–50 on a 100 t capacity hydraulic press.

Each compact was applied with the compressive loading in step of 0.01MN (one metric ton) until the appearance of first visible cracks on the free surface. No lubricant was used for axial deformation. Immediately after the completion of each step of loading, the deformed height, the contact diameters, the bulged diameters and the density were measured. The axial stress (σ_z) is used for the calculation of strength coefficient (K_i) and strain hardening exponent (n_i) for the case of uniaxial stress condition and the hoop stress (σ_θ) is used for the case of plane stress state conditions.

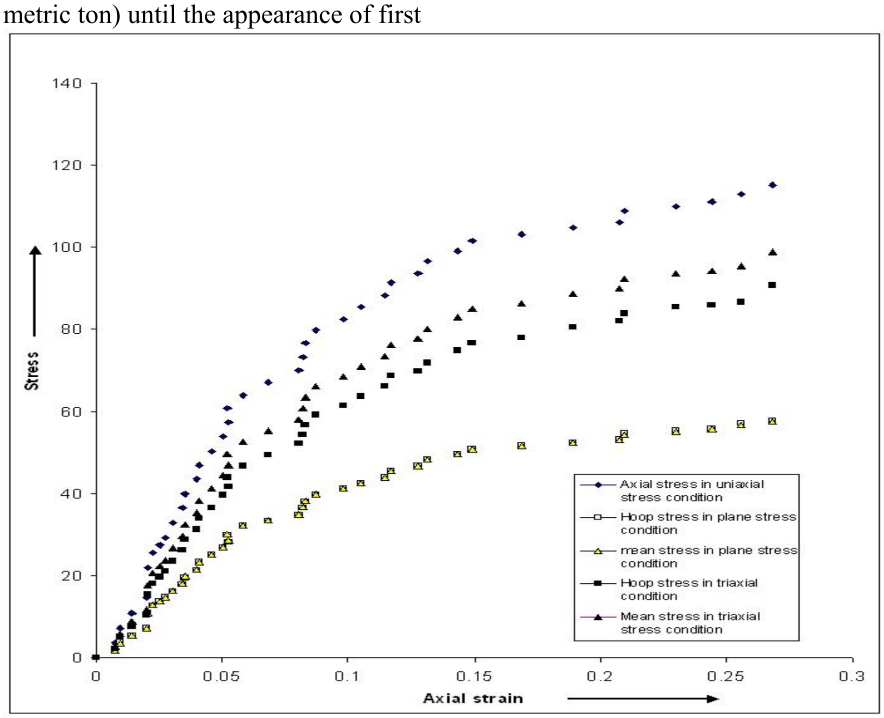

(a)

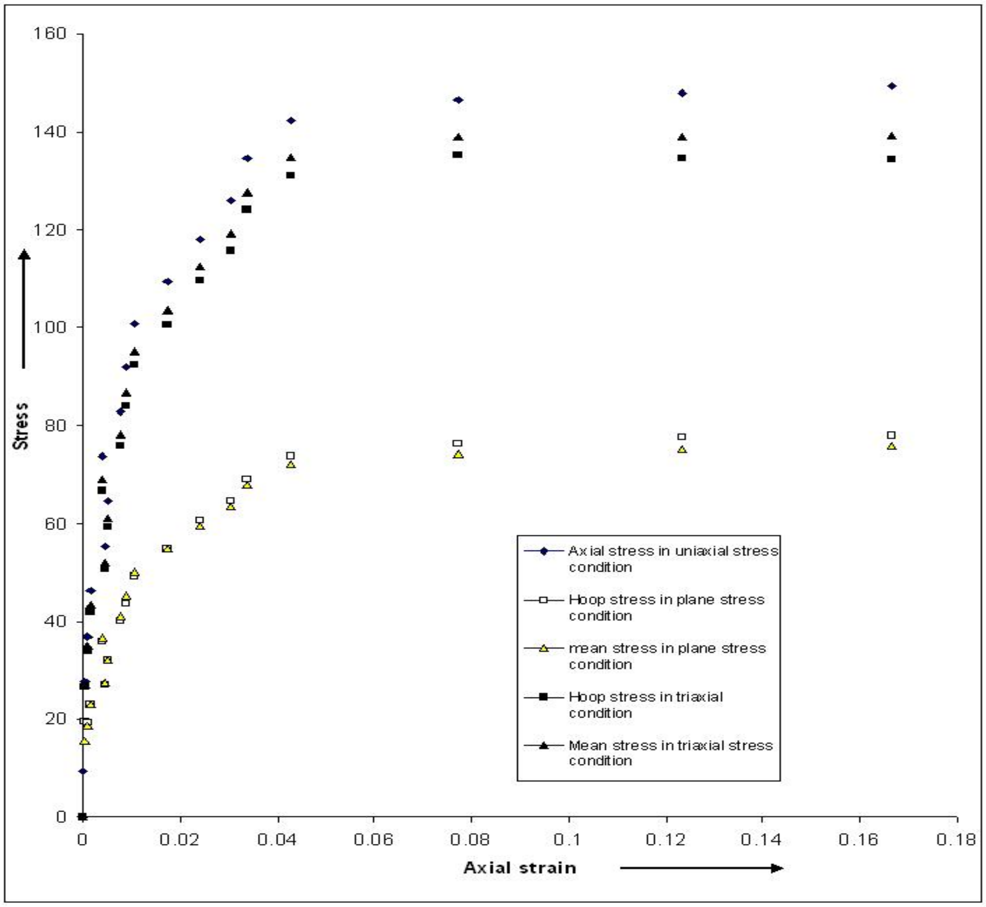
Stress
Axial strain
Axial stress in uniaxial stress condition
Hoop stress in plane stress condition
mean stress in plane stress condition
Hoop stress in triaxial condition
Mean stress in triaxial stress condition

(b)

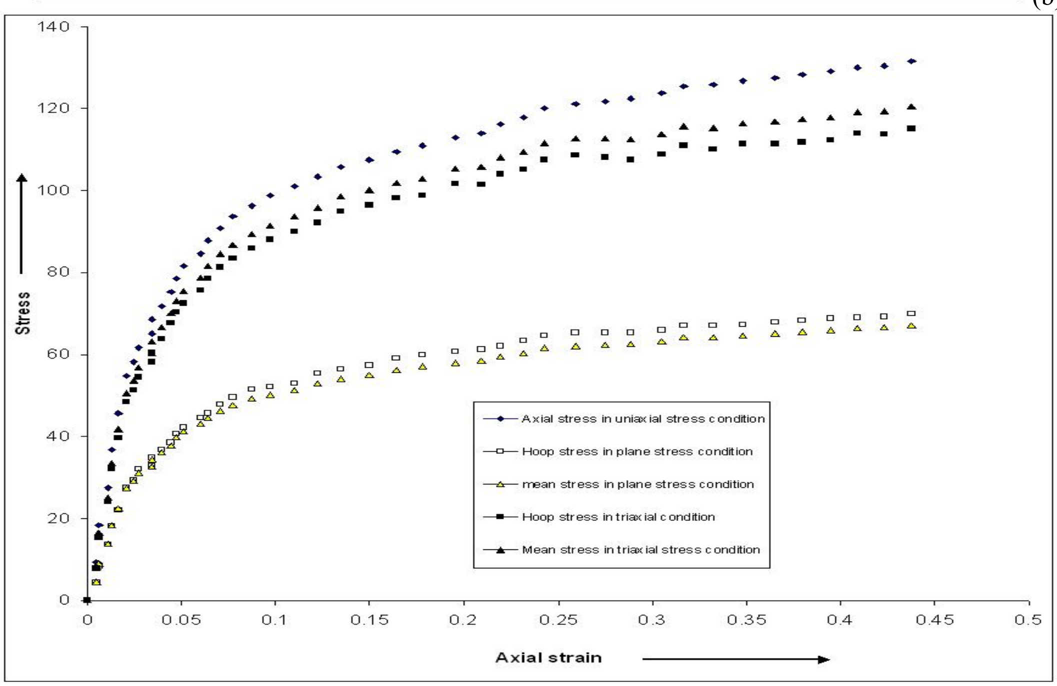
Stress
Axial strain
Axial stress in uniaxial stress condition
Hoop stress in plane stress condition
mean stress in plane stress condition
Hoop stress in triaxial condition
Mean stress in triaxial stress condition

(c)

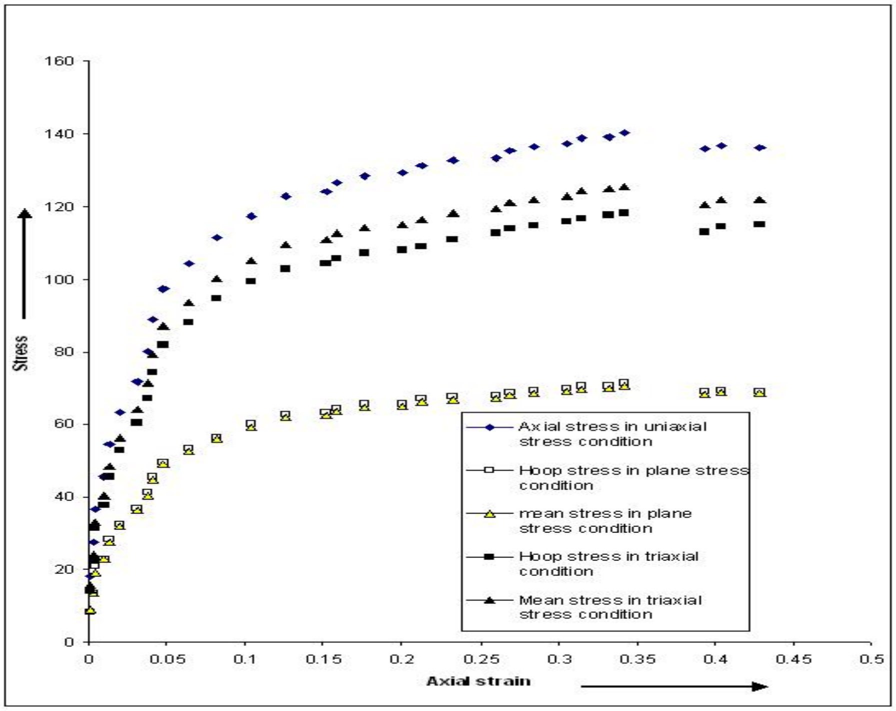
Stress
Axial strain
Axial stress in uniaxial stress condition
Hoop stress in plane stress condition
mean stress in plane stress condition
Hoop stress in triaxial condition
Mean stress in triaxial stress condition

(d)

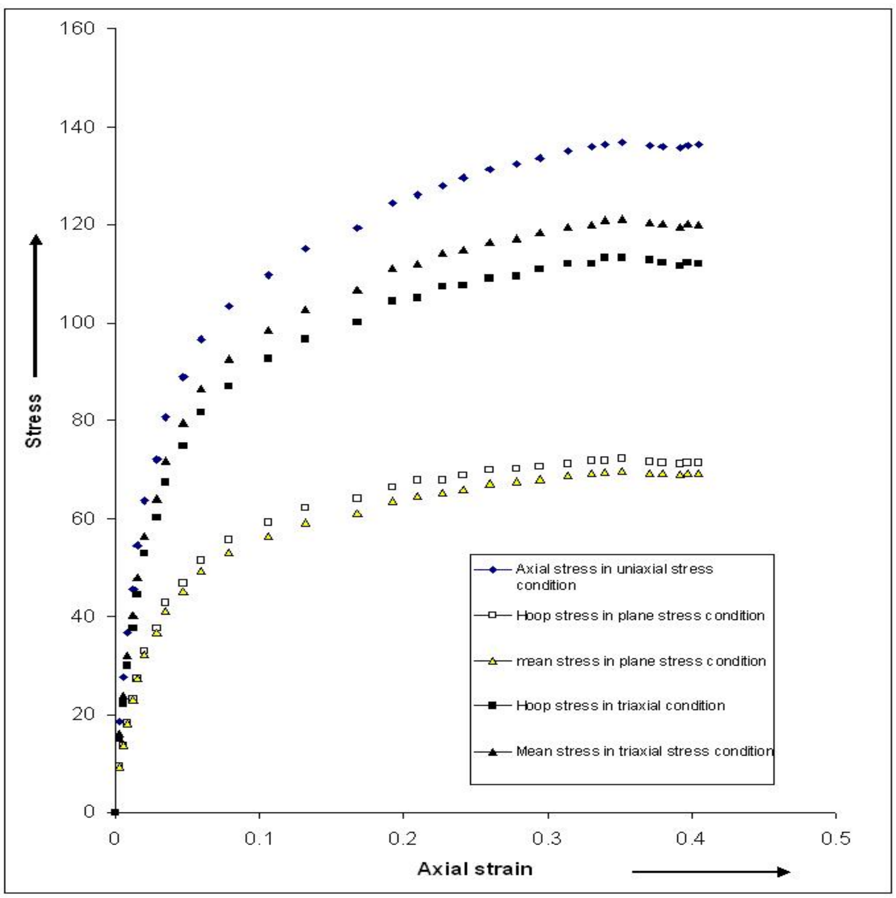
Stress
Axial strain
Axial stress in uniaxial stress condition
Hoop stress in plane stress condition
mean stress in plane stress condition
Hoop stress in triaxial condition
Mean stress in triaxial stress condition

(e)

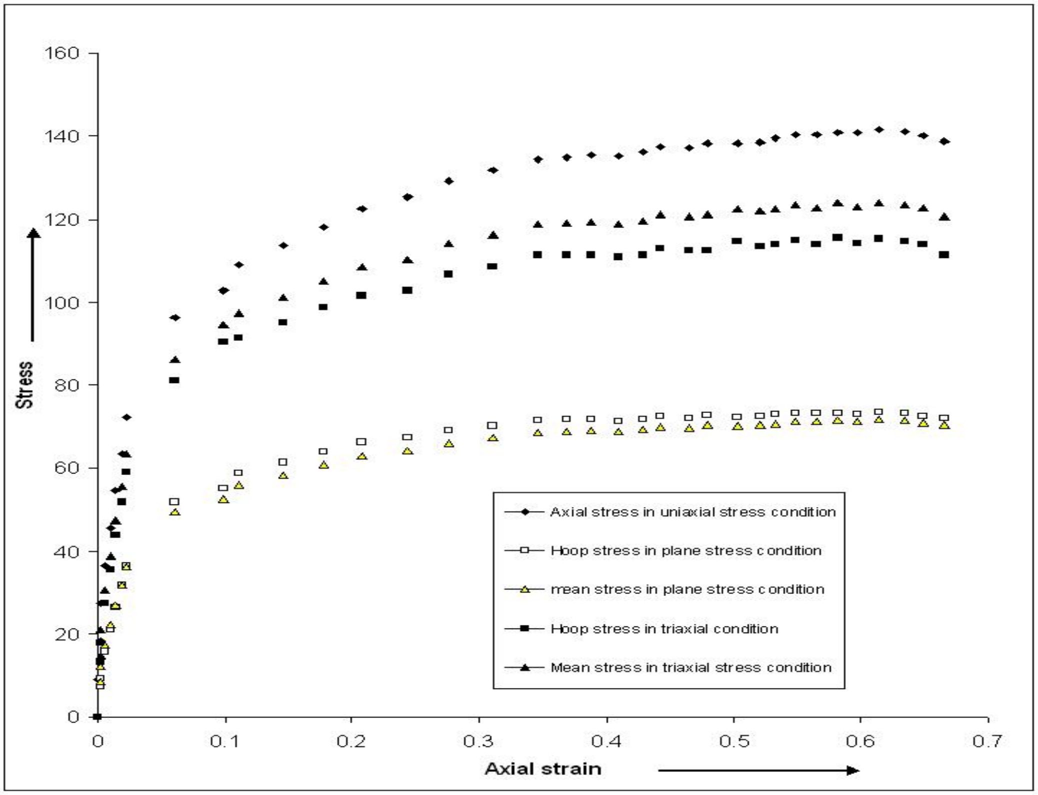
Stress
Axial strain
Axial stress in uniaxial stress condition
Hoop stress in plane stress condition
mean stress in plane stress condition
Hoop stress in triaxial condition
Mean stress in triaxial stress condition

(f)

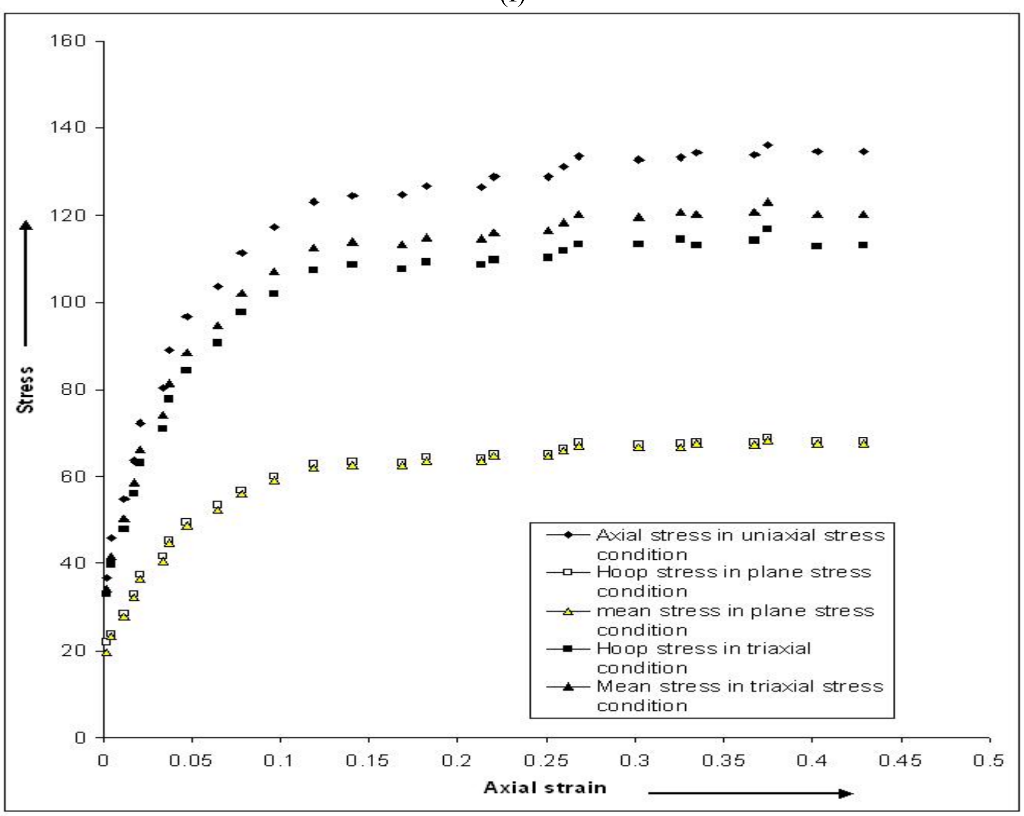
Stress
Axial strain
Axial stress in uniaxial stress condition
Hoop stress in plane stress condition
mean stress in plane stress condition
Hoop stress in triaxial condition
Mean stress in triaxial stress condition

(g)

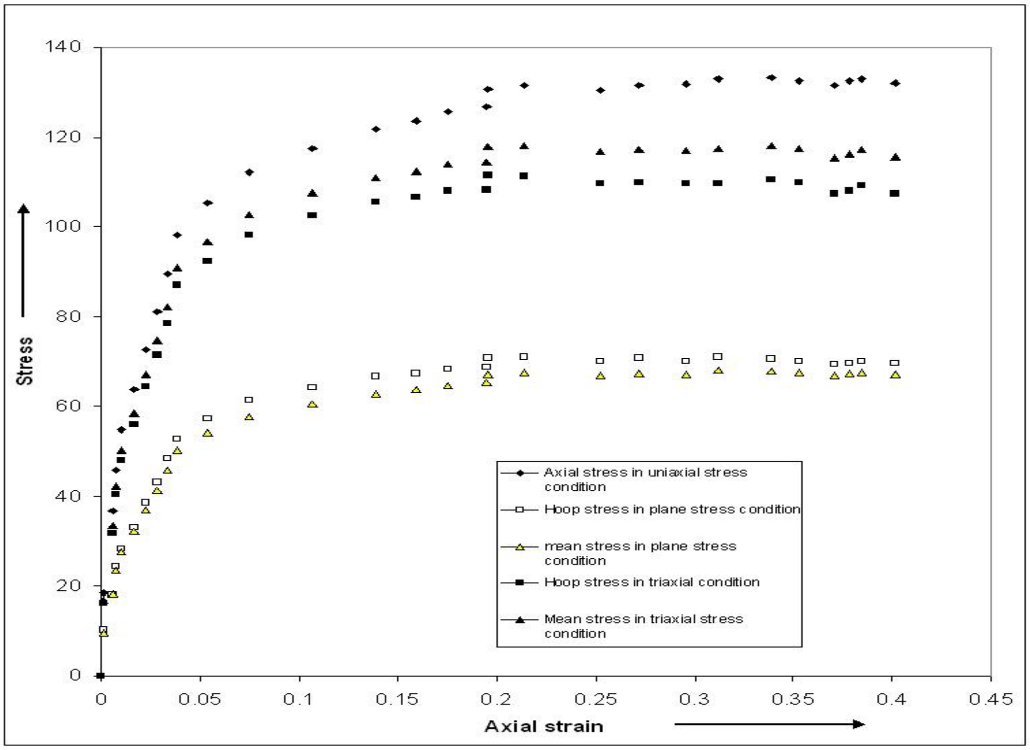
Stress
Axial strain
Axial stress in uniaxial stress condition
Hoop stress in plane stress condition
mean stress in plane stress condition
Hoop stress in triaxial condition
Mean stress in triaxial stress condition

(h)

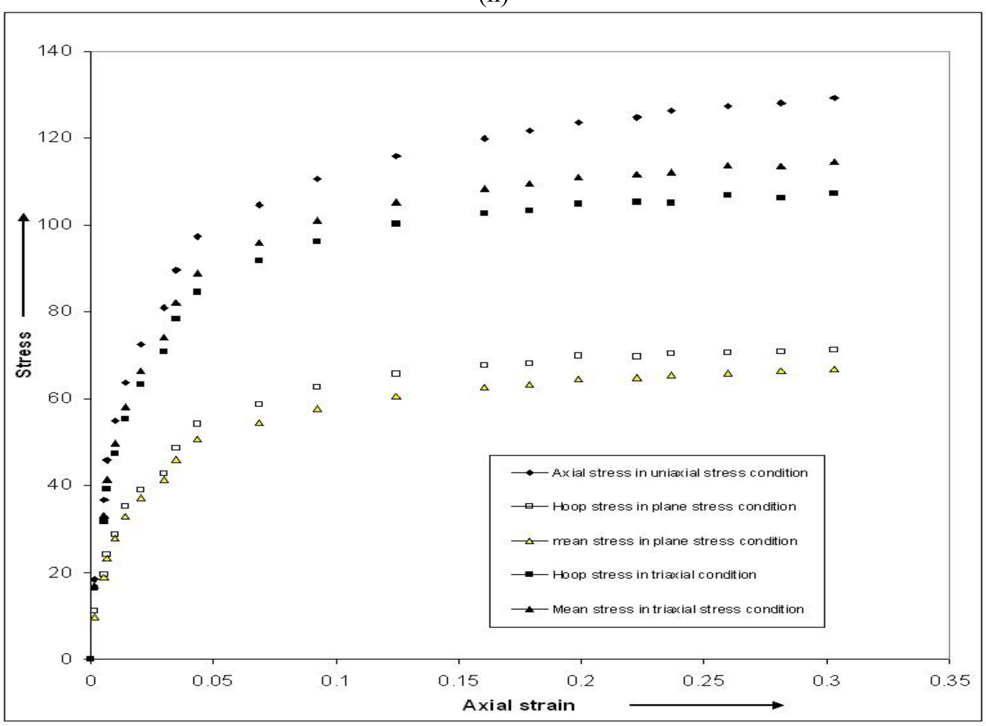
Stress
Axial strain
Axial stress in uniaxial stress condition
Hoop stress in plane stress condition
mean stress in plane stress condition
Hoop stress in triaxial condition
Mean stress in triaxial stress condition

(i)

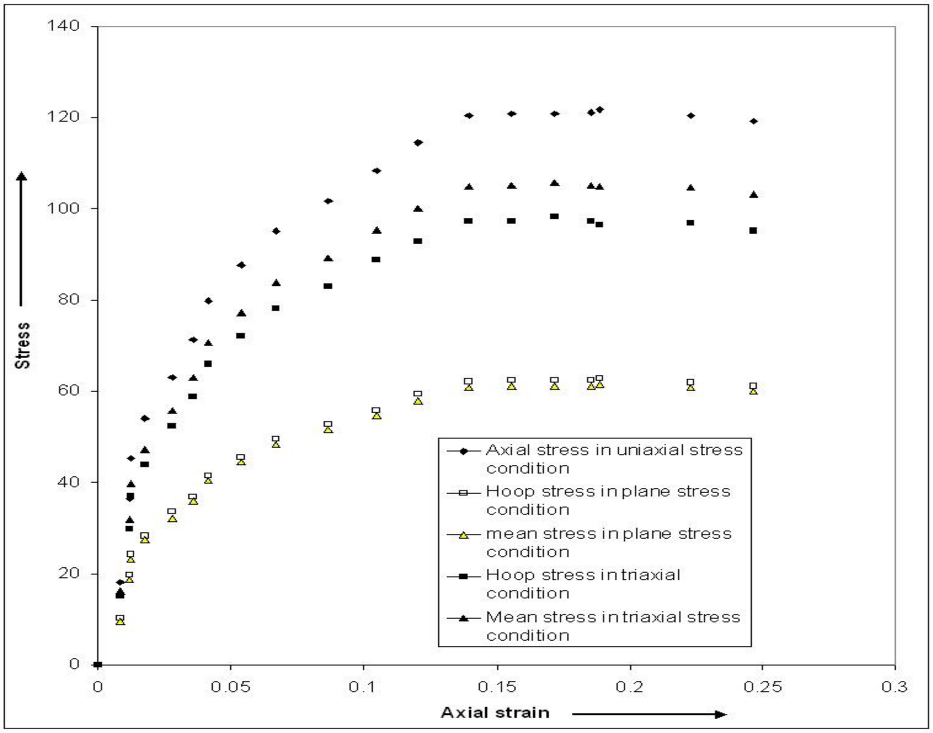
Stress
Axial strain
Axial stress in uniaxial stress condition
Hoop stress in plane stress condition
mean stress in plane stress condition
Hoop stress in triaxial condition
Mean stress in triaxial stress condition

(j)

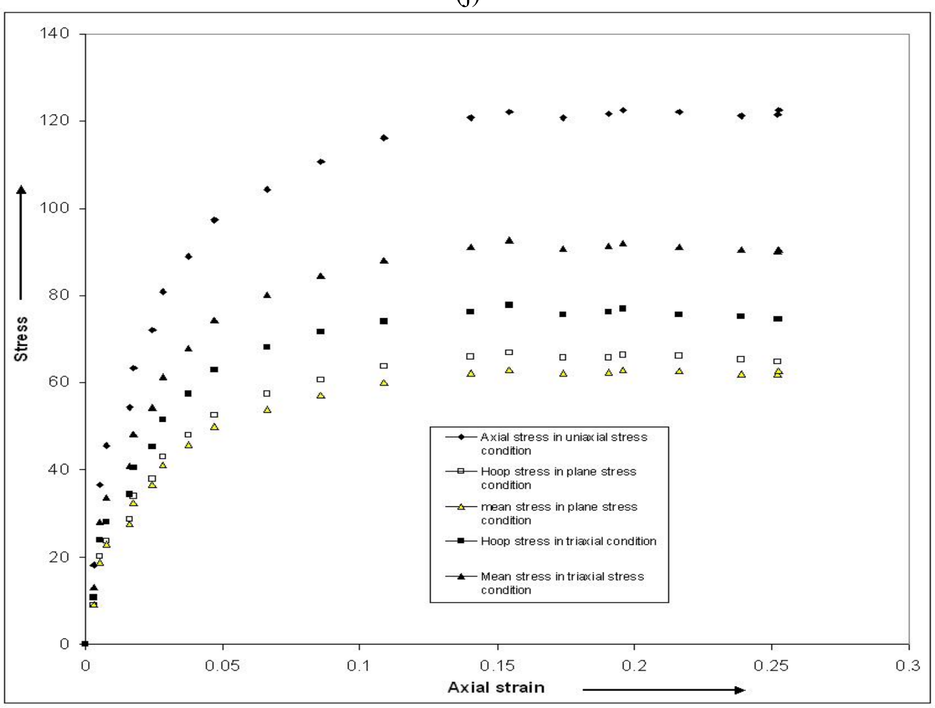
Stress
Axial strain
Axial stress in uniaxial stress condition
Hoop stress in plane stress condition
mean stress in plane stress condition
Hoop stress in triaxial condition
Mean stress in triaxial stress condition

(k)

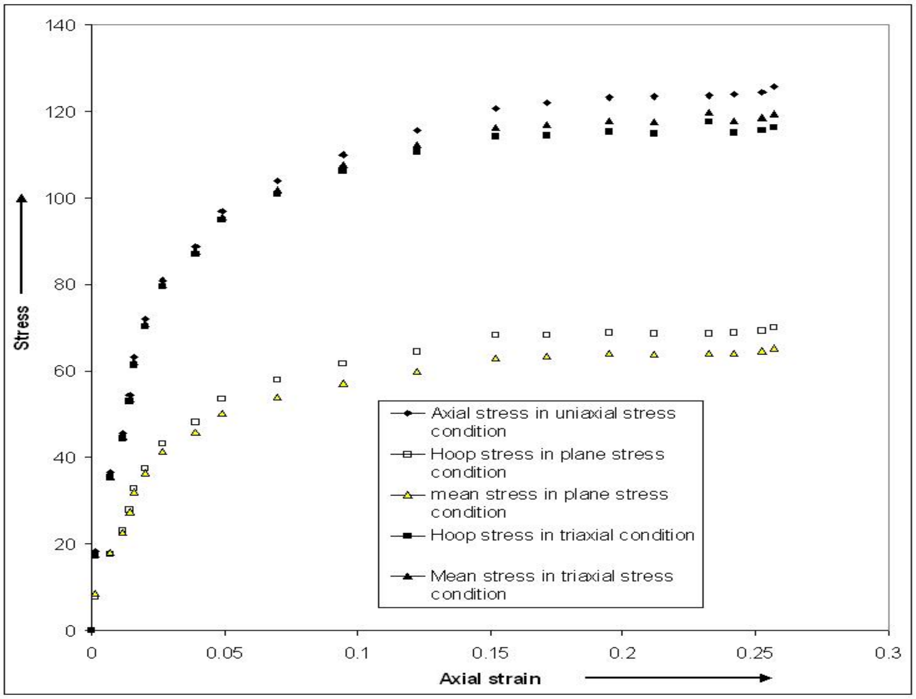

(l)

Fig. 2. (a-c) Various stresses vs. axial strain for Al–0% SiC composite; (d-f) various stresses vs. axial strain for Al–5% SiC composite; (g-i) various stresses vs. axial strain for Al–10% SiC composite; (j-l) various stresses vs. axial strain for Al–15% SiC composite;

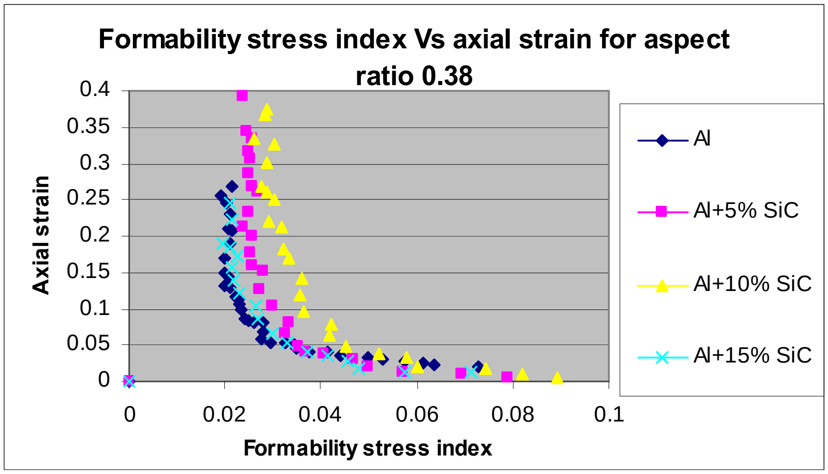

(a)

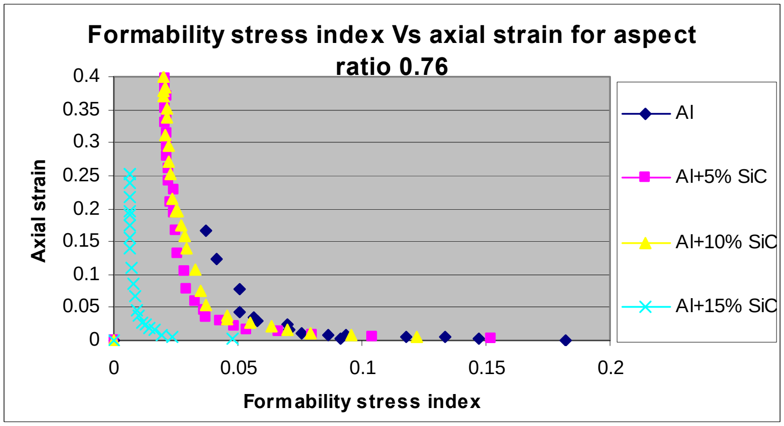

(b)

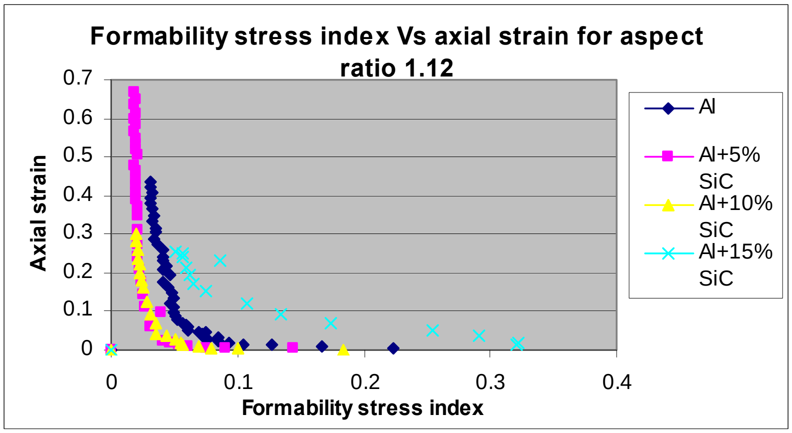

(c)

Fig. 3 (a-c) Axial strain (ε_z) vs. formability stress index β – triaxial stress state condition for various aspect ratios

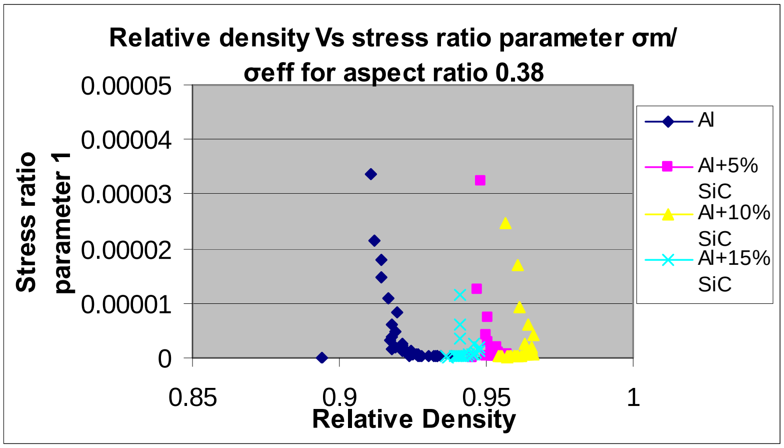

(a)

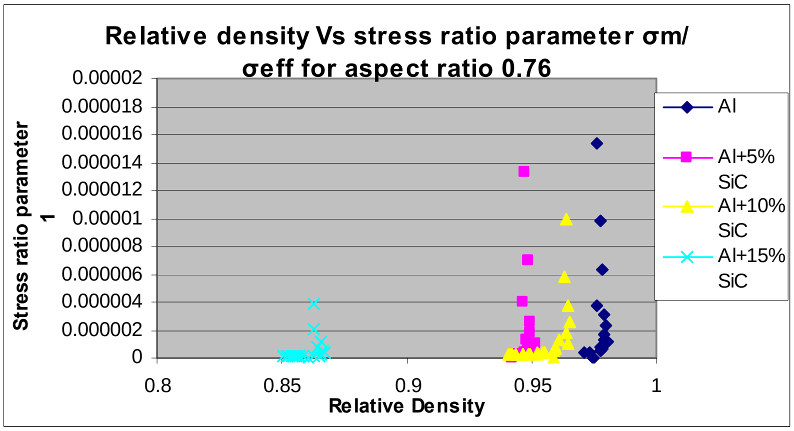

(b)

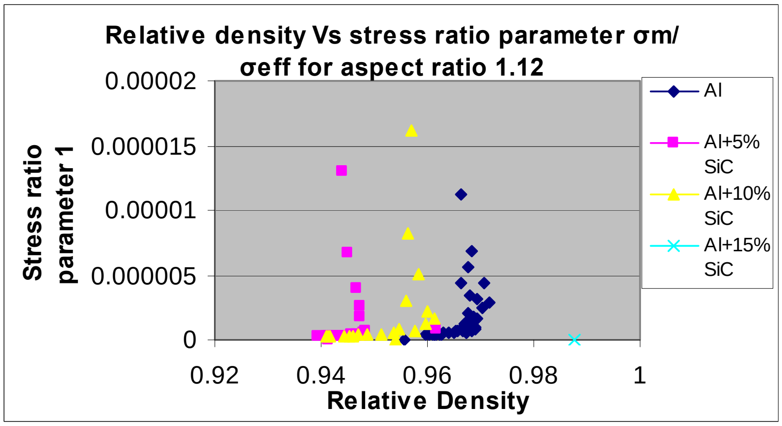

(c)

Fig. 4 (a-c) Stress ratio parameter (σm/σeff) vs. relative density (*R*).

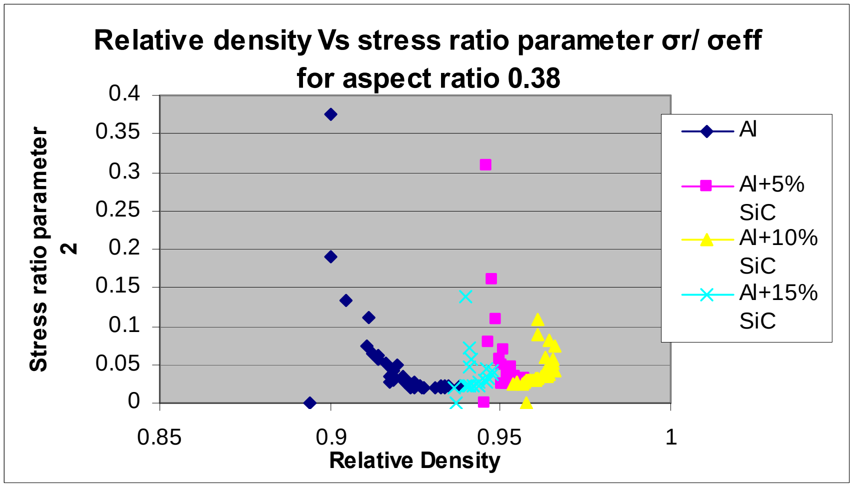

(a)

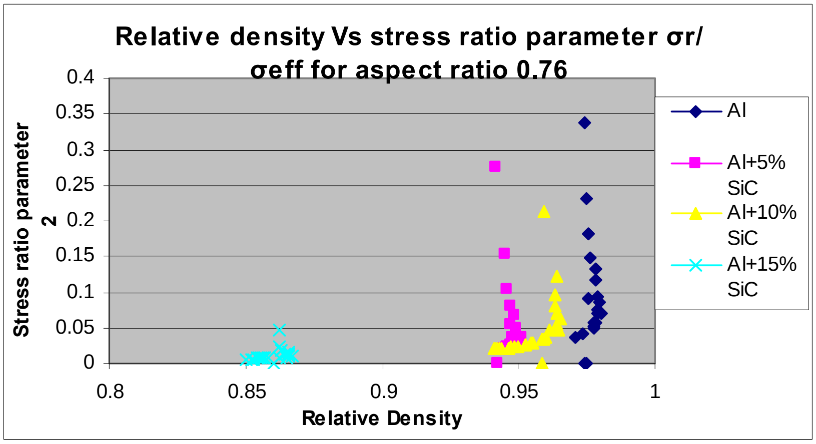

(b)

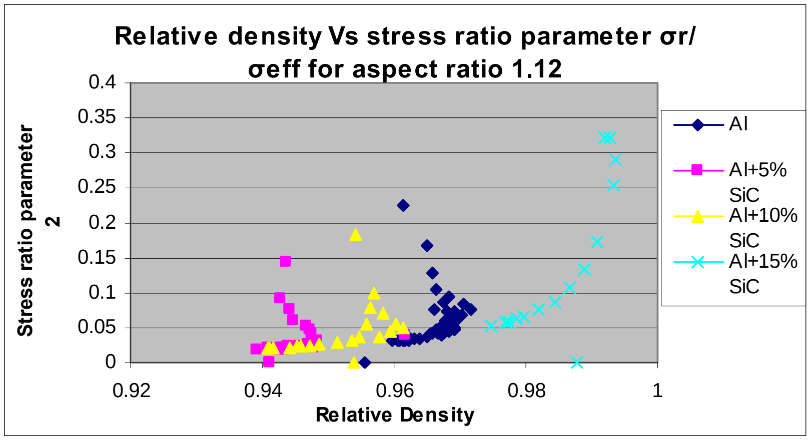

(c)

Fig. 5 (a-c) Stress ratio parameter ($\sigma r/\sigma eff$) vs. relative density (*R*).

IV. RESULTS AND DISCUSSION

Fig. 2(a)–(f) have been plotted between the stresses namely axial–uniaxial, hoop-plane stress, hoop–triaxial, mean-plane stress and mean–triaxial and axial strain (ez) for different SiC content ranging from 0 to 15%. When the SiC addition is made, then all the above stresses and the axial strain (ε_z) value increase. It is also observed that hoop stresses according to plane stress and the axial stress value increase with the increase in SiC addition in the composite. The hydrostatic stress value according to triaxial stress condition increases with an increase in SiC addition. But, this value is less when comparing with compact with no addition of SiC.

Here upto 10% SiC addition the axial stress and triaxial stresses namely hoop stress as well as mean stress are slightly higher than 120 MPa even upto 140 MPa recorded but addition of more silicon carbnide particles above this levcel shows reduction in the stress level, this may due to the particle size which we selected is higher so the void closure may be the reason for this reductions.

REFERENCES

[1] M. Abdel-Rahman, M.N. El-Sheikh, Workability in forging of powder metallurgy compacts, Journal of Materials Processing Technology, Vol.54, 1995, pp. 97-102.

[2] R. Narayanasamy, K S. Pandey, Some aspects of work hardening in sintered aluminium–iron composite preforms during cold axial forming, *Journal of Materials Processing Technology, Vol.* 84, 1998, pp.136–142.

[3] R. Narayanasamy, K S. Pandey, salient features in the cold upset-forming of sintered aluminum-3.5% alumina powder composite preforms, *Journal of Materials Processing Technology*, vol. 72, 1997, pp. 201-207.

[4] J. Bensam, P. Marimuthu, M. Prabhakar, V. Anandakrishnan, Effect of Sintering temperature on the Formability and Pore Closure Behavior of Al-SiC matrix P/M composite, *Applied Mechanics and Materials,* Vol.392, 2013, pp.24-30.

[5] R. Narayanasamy, T. Ramesh, K.S. Pandey, Some aspects on workability of aluminium–iron powder metallurgy composite during cold upsetting, *Materials Science and Engineering*, Vol. A 391,2005, pp. 418–426

[6] R. Narayanasamy, T. Ramesh, K.S. Pandey, Some aspects on strain hardening behaviour in three dimensions of aluminium–iron powder metallurgy composite during cold upsetting, *Materials and Design*, Vol. 27, 2006, pp. 640–650.

[7] Sridhar and N. A. Fleck, Yield behaviour of cold compacted composite powders, *Acta mater.* , Vol.48, 2000, pp. 3341-3352.

[8] Yong li and f. A. Mohamed, An investigation of creep behavior in an SiC-2124 Al composite, *Acta mater*. Vol. 45, No. 11, pp. 4775-4785,

[9] Zhigang Lin, Yong Li, Farghalli A. Mohamed, Creep and substructure in 5 vol.% SiC–2124 Al composite, *Materials Science and Engineering*, Vol. A332, 2002, pp. 330–342.